To provide a bit of context, we're using Paco's HADES and Quijote simulations for the analysis. HADES are the simulations from Paco's (and your) 2018 paper: 100 realizations at different ($\sum m_\nu$, σ_8) pairs. Quijote is Paco's new suite of sims that has 15,000 realizations at a fiducial cosmology and 6,500 more realizations run with all the parameters $(\Omega_{\rm m}, \Omega_{\rm b}, h, n_s, \sigma_8, \sum m_\nu)$ fixed but changing one to either higher or lower than the fiducial value. This is to calculate the derivatives for Fisher forecasts. All of the realizations are 1 h^{-1}Gpc periodic boxes at $z = 0$. The analysis is for halo bispectrum where we impose a $M_h > 3.2 \times 10^13\ M_\odot/h$ limit. The number densities of the realizations are $\sim 1.5 \times 10^{-4}$.

First, here are the redshift-space halo bispectrum $B(k_1, k_2, k_3)$ plots for the HADES simulations: the shape dependence in Figure 1 and the amplitude in Figure 2. More importantly, in Figure 3 we plot the shape-depenence of the $\sum m_\nu$ and σ_8 impact on the bispectrum. The top and bottom panels algined in the three leftmost columns have almost the same CDM+baryon σ_8. Similarly, in Figure 4, we plot the amplitude of the $\sum m_\nu$ and σ_8 impact on the bispectrum. Figures 3 and 4 illustrate that the imprint of $\sum m_\nu$ is more distinguishable from σ_8 in the bispectrum than in the powerspectrum.

Next we use the Quijote simulation suite to calculate the Fisher matrix and forecast $\sum m_\nu$ constraints. In Figure 6, we plot the constraints on the cosmological parameters from the Fisher forecast for the powerspectrum monopole (blue) and bispectrum (orange) over the ranges $k < 0.5$ and $0.01 \leq k_1, k_2, k_3 \leq 0.5$, respectively. The bispectrum substantially improves all the constraints. For $\sum m_\nu$, the bispectrum improves constraints from $\sigma_{\sum m_\nu} = 0.279$ to 0.0258, which is over an order of magnitude improvement. In Figures 7 and 8, we plot the Fisher forecast constraints for $k_{\rm max} = 0.2, 0.3, 0.5$. Regardless of $k_{\rm max}$, the bispectrum improves the $\sum m_\nu$ constraint by roughly an order of magntiude.

Here's a few tests we've run to check our results:

- We've tested the convergence of the covariance matrix by calculating the Fisher constraints where we estimate the covariance matrix with different number of Quijote simulations. We find that the constraints converge after $\sim 10,000$ mocks.
- We've also tested the convergence of the derivatives $\frac{\partial B}{\partial \theta_i}$ by varying the number of Quijote simulations. Although we have 15,000 realizations at the fiducial parameter, for the derivatives we only have 500. Still, we find only small changes $< 10\%$ in the constraints from using 400 to 500.
- We've calculated $\Delta\chi^2$ values for the HADES simulations and they're in agreement with the contours that we find.
- We've also run the Fisher forecasts using select triangle configurations, such as equilateral and squeezed, for different $k_{\rm max}$. We find that the improvements on $\sum m_\nu$ saturate at $k_{\rm max} \sim 0.4$, which correctly corresponds to the scale where we find that shot noise dominates.

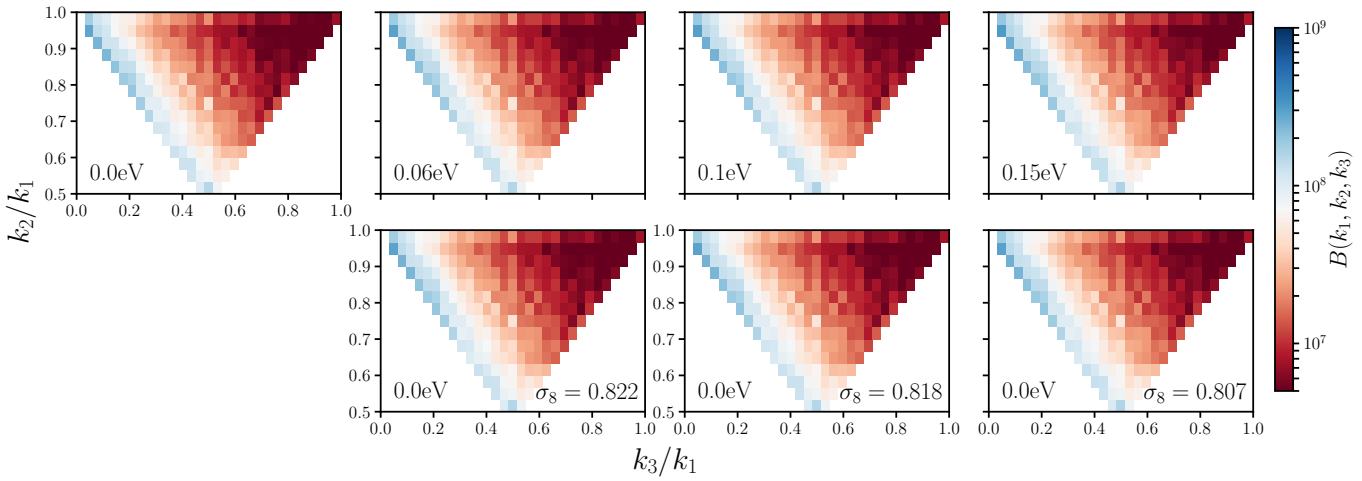

Figure 1. The redshift-space halo bispectrum, $B(k_1, k_2, k_3)$ as a function of triangle configuration shape for $\sum m_\nu = 0.0, 0.06, 0.10$, and $0.15\,\mathrm{eV}$ (top panels) and $\sigma_8 = 0.822, 0.818, 0.807$, and 0.798 (lower panels). We include all triangle configurations within the k range: $0.01 \leq k_1, k_2, k_3 \leq 0.5$.

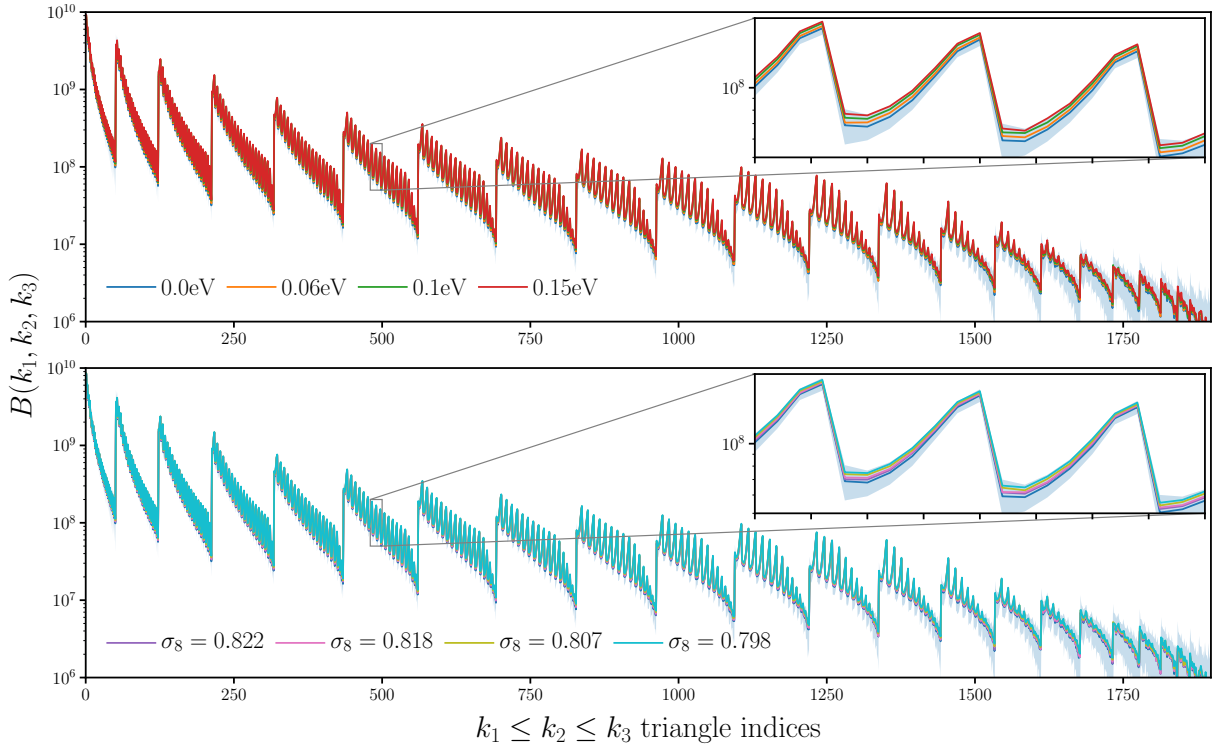

Figure 2. The redshift-space halo bispectrum, $B(k_1, k_2, k_3)$, as a function of all triangle configurations within $0.01 \leq k_1, k_2, k_3 \leq 0.5$. for $\sum m_\nu = 0.0, 0.06, 0.10$, and $0.15\,\mathrm{eV}$ (top panel) and $\sigma_8 = 0.822, 0.818, 0.807$, and 0.798 (lower panel). The triangle configurations are ordered such that $k_1 \leq k_2 \leq k_3$, the same ordering as Hector's plots. The shaded region in plots the uncertainties from the covariance matrix estimated from the Quijote simulations (Figure 5).

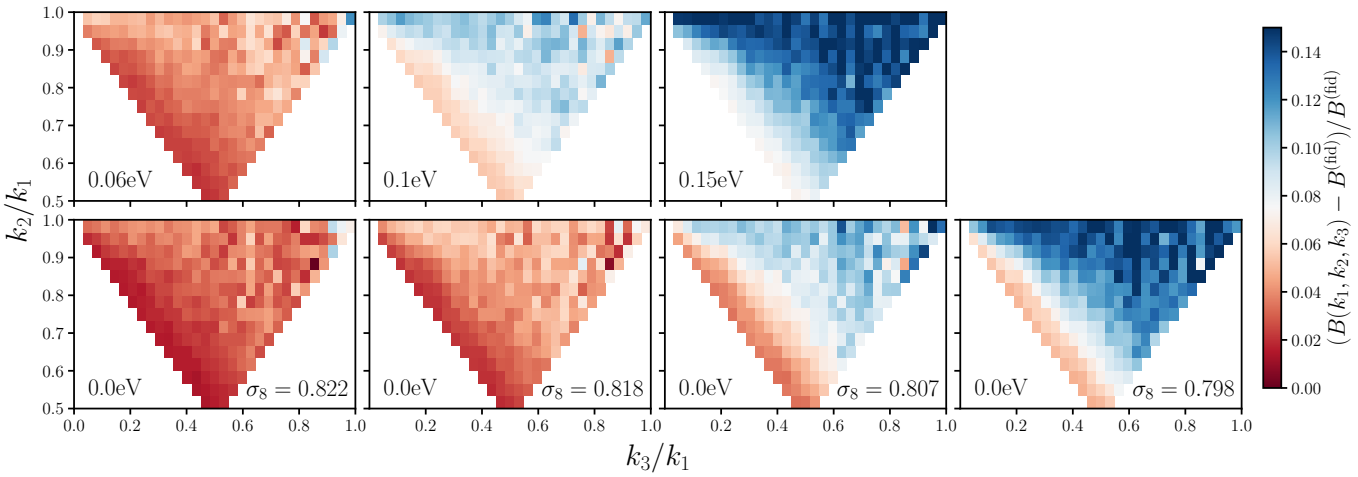

Figure 3. The shape dependence of the impact $\sum m_\nu$ and σ_8 have on the redshift-space halo bispectrum, $\Delta B/B^{(\mathrm{fid})}$. $\sum m_\nu = 0.06, 0.10$, and $0.15\,\mathrm{eV}$ (top panels; left to right) are aligned with $\sigma_8 = 0.822, 0.818$, and $0.807\,\mathrm{eV}$ (bottom planes; left to right). In each of the three leftmost columns, the top and bottom panels have matching CDM + baryon σ_8, which produce mostly degenerate imprints on the redshift-space power spectrum. The differences between the top and bottom panels in every column illustrate that $\sum m_\nu$ *induces a sigificantly different impact on the shape-dependence of the halo bispectrum than* σ_8.

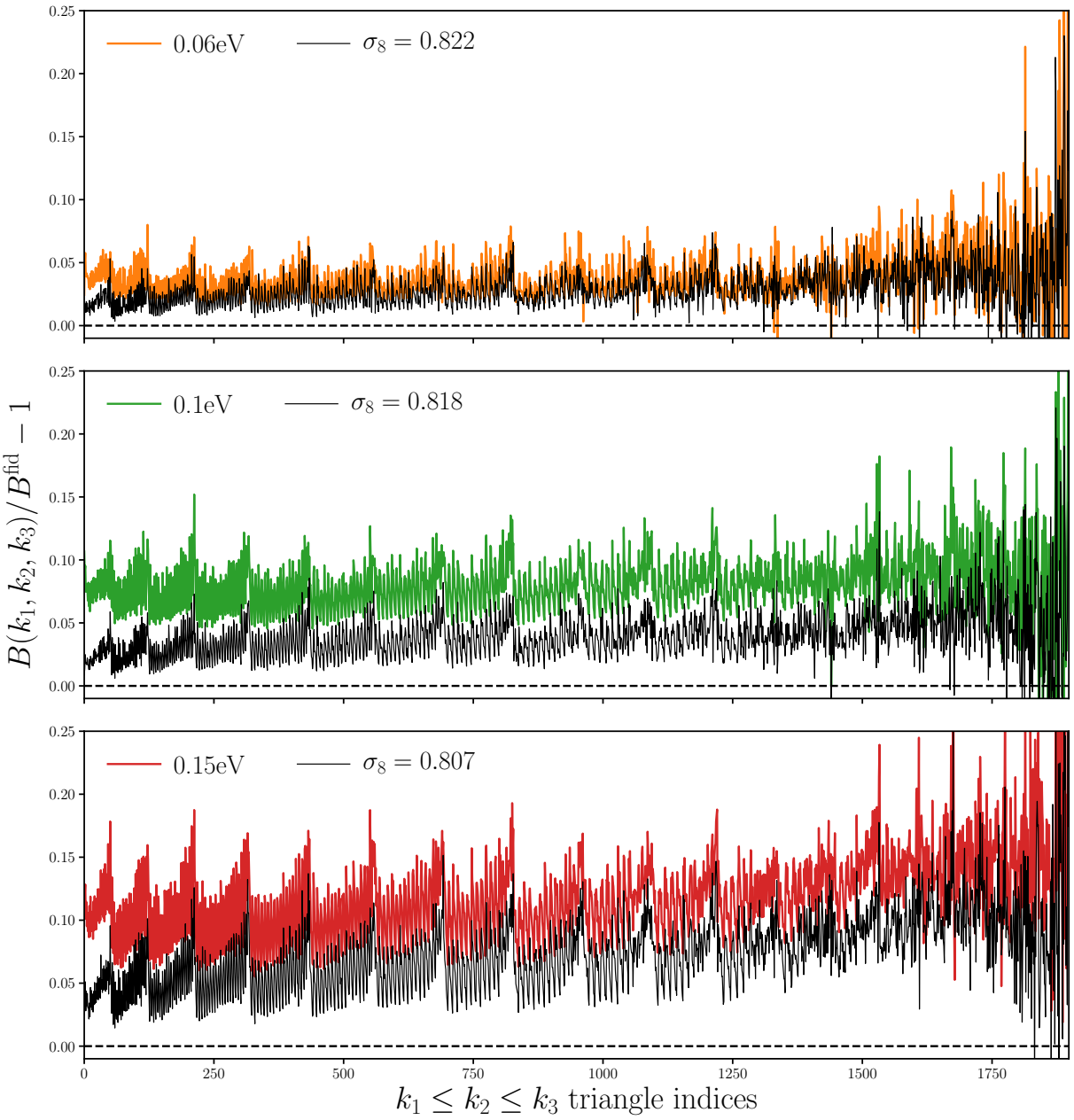

Figure 4. The impact of $\sum m_\nu$ and σ_8 on the redshift-space halo bispectrum for all triangle configurations within $0.01 \leq k_1, k_2, k_3 \leq 0.5$: $\Delta B/B^{(\rm fid)}$. $\Delta B/B^{(\rm fid)}$s plotted in each panel have matching σ_8 values. The impact of $\sum m_\nu$ differs significantly from the impact of σ_8 both in amplitude and scale dependence. For instance, in the bottom panel, $\sum m_\nu = 0.15\,$eV (red) has a $\sim 5\%$ larger impact on the bispectrum than $\sigma_8 = 0.807$ (black). Combined with the shape-dependence of Figure 3, *the contrasting impact of* $\sum m_\nu$ *and* σ_8 *on the redshift-space halo bispectrum illustrate that the bispectrum break the degeneracy between* $\sum m_\nu$ *and* σ_8 *that degrade constraints from two-point analyses.*

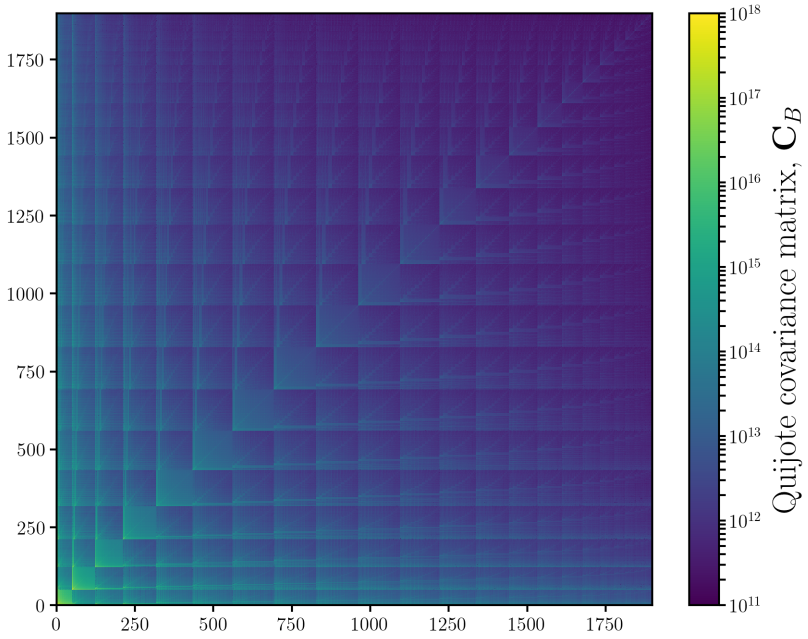

Figure 5. Covariance matrix of the redshift-space halo bispectrum estimated using the 15,000 realizations of the Qujiote simulation suite with the fiducial cosmology: $\Omega_{\rm m}$=0.3175, $\Omega_{\rm b}$=0.049, h=0.6711, n_s=0.9624, σ_8=0.834, and $\sum m_\nu$=0.0 eV. The triangle configurations (the bins) are ordered in the same fashion as Figures 2 and 4.

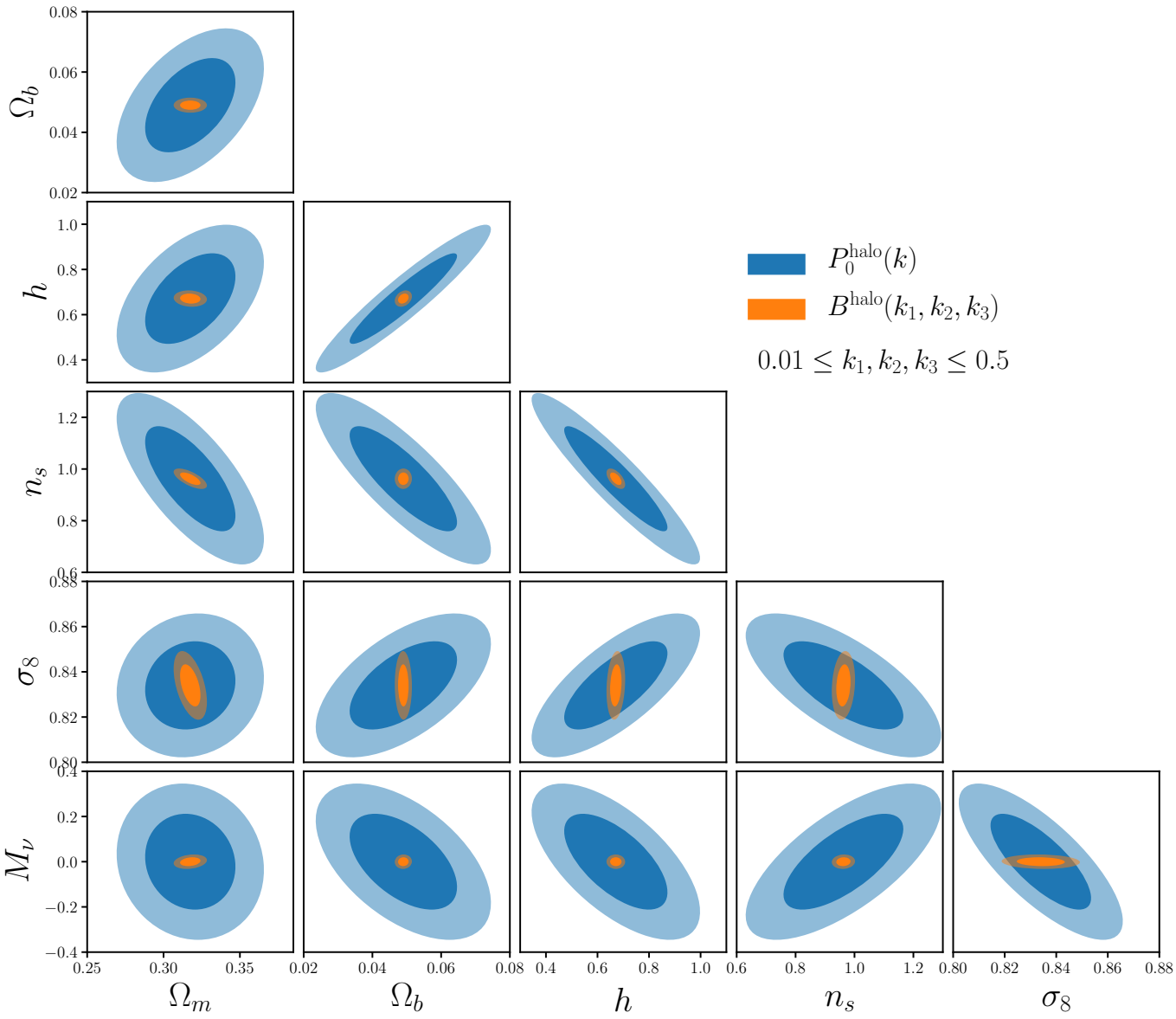

Figure 6. Constraints on cosmological parameters from the redshift-space halo powerspectrum monopole (blue) and bispectrum (orange) derived using Fisher matrices computed from the Quijote simulation suite. For the powerspectrum we include modes with $k \leq 0.5$; for the bispectrum we include triangle configurations with $0.01 \leq k_1, k_2, k_3 \leq 0.5$. The bispectrum *substantially* improves constraints on the cosmological parameters. The improvement over the powerspectrum is particularly evident for $\sum m_\nu$, where the $\sum m_\nu$ constraint improves from $\sigma_{\sum m_\nu} = 0.279$ to 0.0258 with the bispectrum — *over an order of magnitude improvement.*

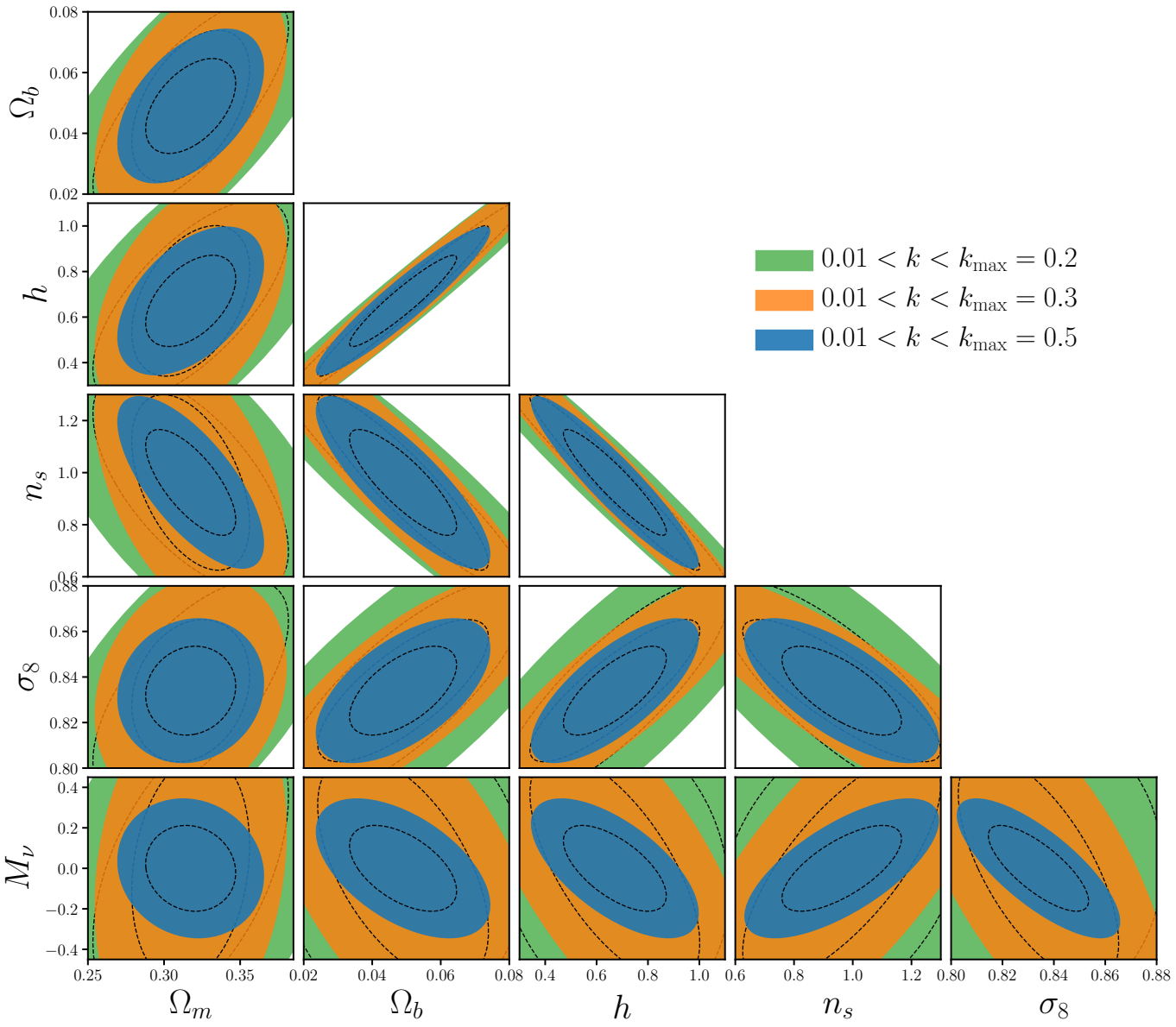

Figure 7. Constraints on cosmological parameters from the redshift-space halo powerspectrum monopole for $k_{\rm max} = 0.2$ (green) 0.3 (orange), and 0.5 (blue).

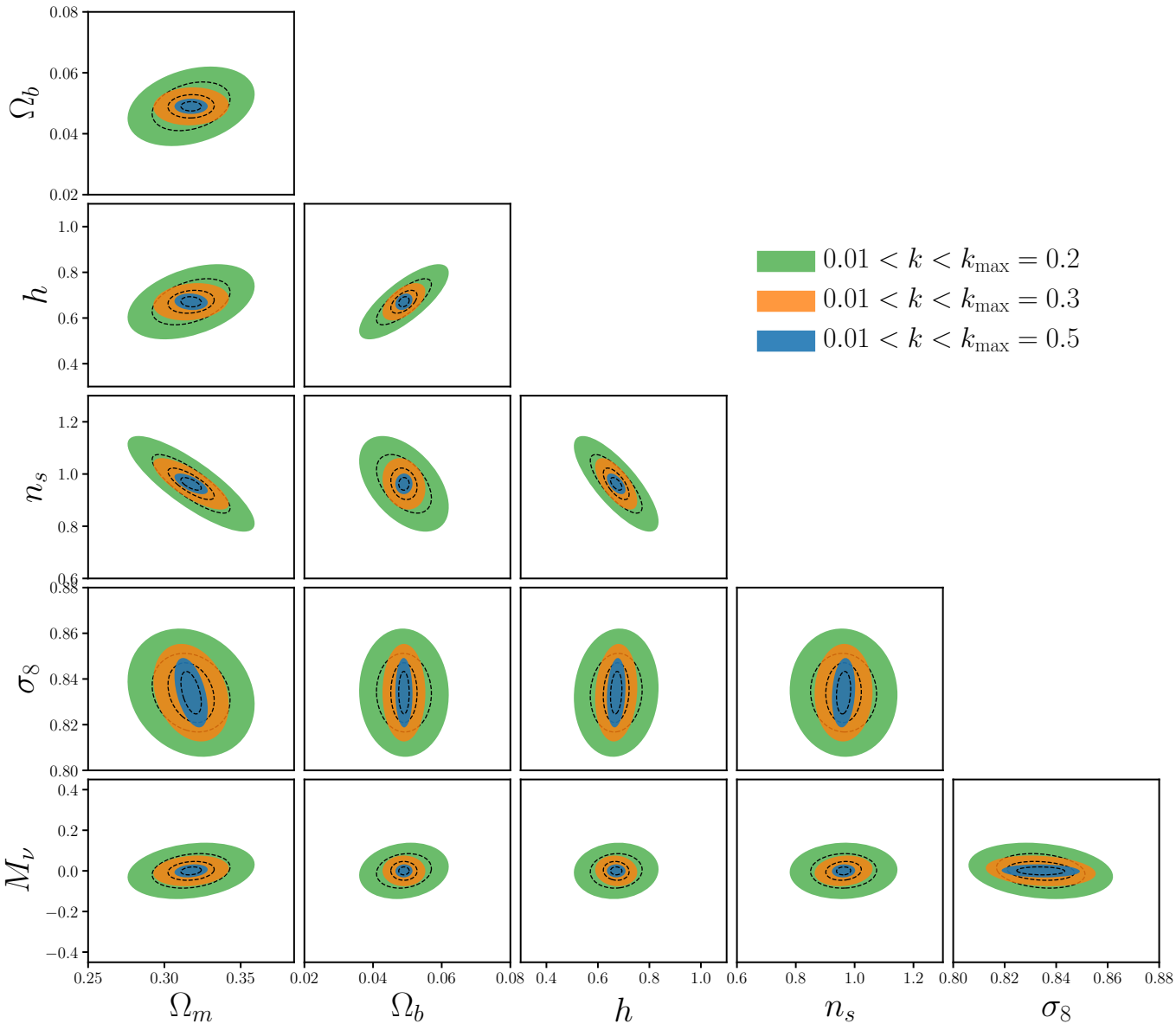

Figure 8. Constraints on cosmological parameters from the redshift-space halo bispectrum for $0.01 \leq k_1, k_2, k_3 \leq k_{\rm max} = 0.2$ (green) 0.3 (orange), and 0.5 (blue).